The microstructure and composition of granulated platinum furnace slags

Lesley ANDREWS[1] and Chris PISTORIUS[2]*

1) Anglo American Technical Solutions–Research, Johannesburg, South Africa.

2) Center for Iron and Steelmaking Research, Carnegie Mellon University, U.S.A.

Abstract: Platinum-bearing concentrates are processed in three South African smelters by Anglo American's Platinum business. The tapped slags from the primary melting furnaces and slag cleaning furnace (SCF) are granulated in high-pressure streams of water. The bulk of the granulated slag consists of amorphous silicate glass which contains trace amounts of entrained matte as sulphide inclusions, as well as slag spinel crystals. Quenched slags such as those used in this study are thought to reflect the conditions and phases present in the molten slags during smelting.

In this study electron probe microanalysis (EPMA) of the glass composition revealed variation within furnace slag as well as between furnace and SCF slag composites. Not only do the results reflect variation in dissolved base metal levels, but they also allow a record of slag chemistries to be compiled and inter-elemental relationships to be examined. Larger SCF slag granules were also selected for study – these contain multiple matte inclusions. Results of glass EPMA of these granules and corresponding entrained matte analysis in the scanning electron microscope (SEM) can be used to demonstrate the degree of equilibrium achieved within the slag, and provide a comparison of base metal partition ratios with those at equilibrium.

Keywords: Platinum slags, Slag composition, Slag mineralogy, Base metal partitioning

1. Introduction

The largest platinum group element reserves in the world are found in South Africa. These metals are mined from the Bushveld Complex in the north west of the country and concentrated ores are processed by smelting and refining [1,2]. The base metals (nickel, copper and cobalt) are also recovered as part of the platinum-producing process.

Anglo American's Platinum business (hereafter referred to as Platinum) operates three smelters, but converting is confined to Waterval Smelter, near Rustenburg. Blended ore concentrate is dried in the flash driers, and then fed into the primary melting furnaces, which are submerged arc electric resistance furnaces. Matte from these furnaces is tapped into ladles and granulated in water, after which it is stored prior to being used as converter feed. Furnace slag is tapped continuously and granulated in water, then dewatered and stored. A portion of this slag is milled and floated, but most of it is dumped.

The purpose of the slag cleaning furnace is to recover valuable base metals from converter slag; because of oxidizing conditions in the converter, the converter slag has a significant concentration of nickel, copper and cobalt (Table 1). The slag cleaning furnace (SCF) treats converter slag by melting this slag with ore concentrate, with addition of carbon as reductant. SCF slag is also granulated in water and is further treated by slag milling and flotation. These processes, as

well as others at the smelter, have been described in detail [3,4]. The process flow at Waterval Smelter is shown in Figure 1.

This paper describes the latest advances in the microanalysis of granulated primary furnace slag and SCF slag, specifically intragranular (i.e., within slag granules) electron probe micro-analysis (EPMA) results. EPMA to determine dissolved (or chemically-bound) base metals in furnace slag has been used in combination with automated scanning electron microscope (SEM) analysis of mechanically entrained matte phases in the slag to describe base metal distribution in the slag. Previously such data has been used to investigate departure from equilibrium in the primary smelting furnaces [5], and the results for a slag cleaning furnace are described below. In the case of the primary smelting furnace slag, it was found that the concentrations of dissolved base metal oxides appear to equilibrate with the entrained matte droplets in the slag (and not with the bulk tapped matte); the work described here tested whether the same held for the slag cleaning furnace, despite the very different composition of the slag cleaning furnace slag (see Table 2), and differences in furnace design.

Figure 2 gives an approximate mass balance for the slag cleaning furnace. Not shown in the mass balance are the small amount of carbon fed (approximately 1.9% of the mass of the converter slag feed), and the off-gas. The mass balance illustrates that nickel recovery to the matte product is approximately 85% (compared with *ca*. 75% for copper and 50% for cobalt). (The inputs labelled "Others" in Figure 2 are various recycled materials, which can be seen to constitute a small part of the furnace input.)

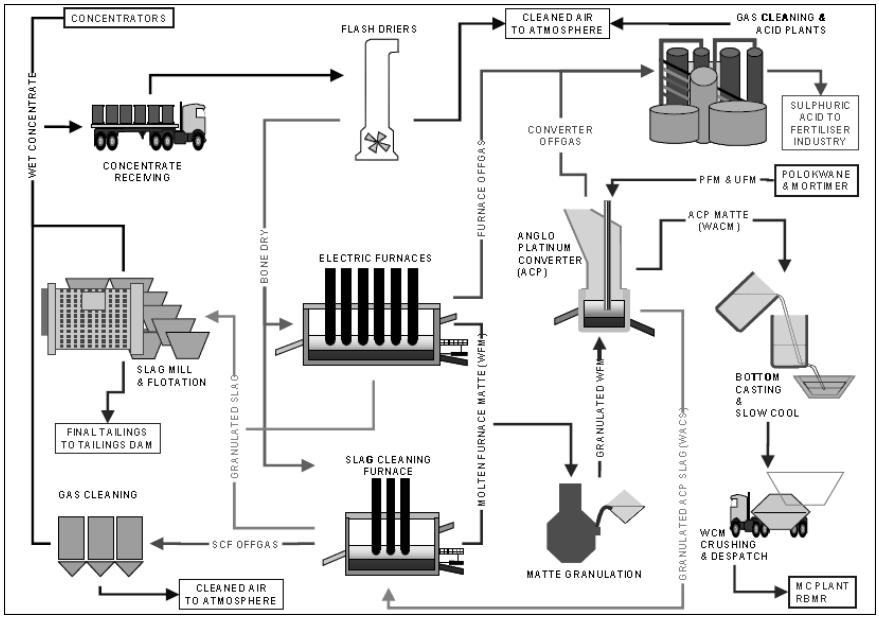

Figure 1. Schematic diagram of process flow at Waterval Smelter (after Jacobs [3] and Hundermark [4])

Table 1. Compositions (mass %) of converter slag and concentrate (main feeds to slag cleaning furnace)

Concentrate	Ni	Cu	Co	Fe	S	SiO_2	MgO	FeO	Al_2O_3	CaO
	1.9	1.4	0.05	8.3	4.9	49.0	18.4	8.8	4.2	2.9

Converter slag	FeO	Fe_2O_3	SiO_2	NiO	Cu_2O	CoO	Al_2O_3	CaS	MgO	MgS
	40.3	22.4	26.9	5.2	2.0	0.65	1.6	0.50	0.31	0.21

2. Experimental

The techniques used during sampling, sample preparation and analysis are shown below.

2.1 Sampling procedures

Daily samples were taken as a cut across the primary furnaces and SCF slag conveyer belts for a period of one month; these were later composited to form two monthly composite samples.

2.2 Sample preparation

The slag samples were dried and split. One split was milled and submitted for chemical analysis, and the other was mounted in resin and polished sections for EPMA analysis were prepared and then carbon coated. In order to collect data for the SCF matte-slag equilibrium modelling, larger SCF slag granules were selected, set in resin and reground twice to expose sufficient entrained matte phases to analyse.

2.3 Non-microbeam techniques

The slag composites were analysed for major and minor elements. The method used was base metal fusion and ICP-MS, apart from sulphur, which was analysed by LECO (combustion).

Mössbauer Spectroscopy was run on bulk samples at North West University in order to determine the Fe^{3+}/Fe^{2+} ratio. Analysis of platinum slags using this technique has been reported previously [6].

2.4 EPMA measurement techniques

EPMA was run on the Cameca SX100 electron microprobe at the University of Johannesburg. The instrument performs quantitative wavelength dispersive X-ray spectroscopy (WDS) analysis and is calibrated with standards. For inter-granular analysis, analysis positions are programmed on the centre of the granules and the beam is defocused to 2 µm (furnace and SCF slag) and 5 µm (SCF slag large granules). During programming, optical focusing and back-scattered electron (BSE) imaging are employed to prevent the points falling on entrained matte phases. More details of platinum slag EPMA techniques are provided in the literature [6,7].

The large SCFS granules were analysed using a combination of energy dispersive X-ray spectroscopy (EDS) on the SEM for the entrained matte phases and EPMA as described above for the surrounding slag silicate.

2.5 Modelling

Equilibrium calculations were performed using the Equilib module of FactSage [8]. More details of the methods used are given in section 3.4.

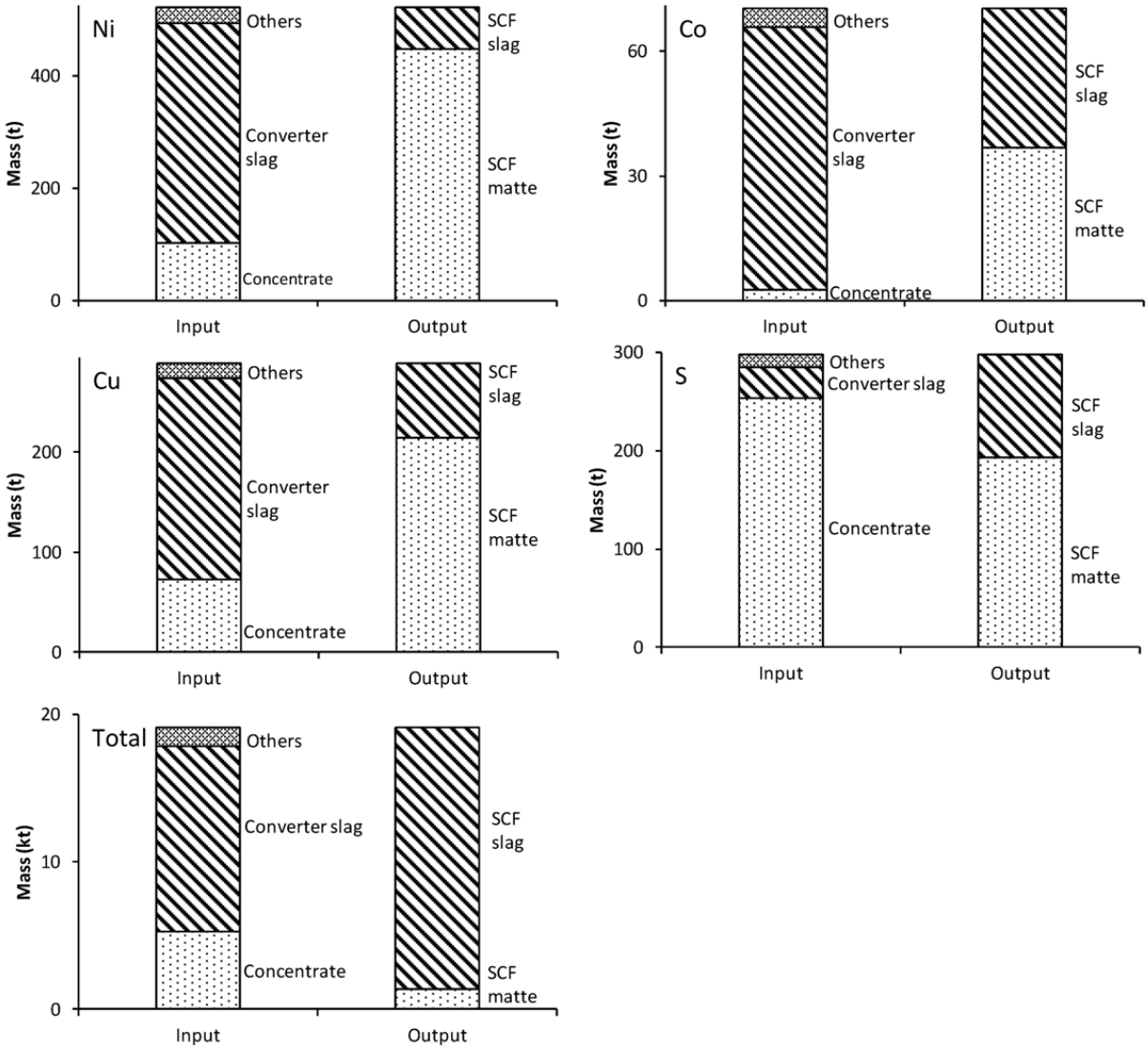

Figure 2. Approximate mass balance for slag cleaning furnace, based on 1 month of operation.

3. Results and Discussion

The results of analysis and modelling are described and discussed in this section.

3.1 Chemical analysis

The results of whole slag chemical analysis are shown in Table 2.

Table 2. Results of chemical analysis of the slag composites in mass %

	Mg	Al	Si	Ca	Cr	Fe	Co	Ni	Cu	S
Primary furnace slag	13.24	3.26	23.54	2.72	1.26	10.20	0.012	0.074	0.032	0.13
SCF slag	4.54	1.92	17.27	1.04	1.33	34.91	0.150	0.340	0.320	0.58

3.2 Mössbauer spectroscopy

The Fe^{3+}/Fe^{2+} ratios of the bulk slag samples were reported as 0.035 (furnace slag) and 0.064 (SCF slag). Both slags are therefore fairly reducing, especially compared with converter slag, in which the Fe^{3+}/Fe^{2+} ratio is approximately 0.5. It should be noted that the accuracy of the determinations is quoted as ± 1% absolute of the Fe^{3+} levels reported in the slag.

3.3 SEM and EPMA results

Granulated slag from the furnaces and the SCF consists predominantly of amorphous silicate glass. Entrained Fe-Ni-Cu sulphide matte is usually present in the glass as spherical inclusions, hence the reference to matte "droplets". Slag spinel ($(Cr,Fe,Mg\pm Al)_3O_4$) crystals may also be present, especially if the slag contains over 2 % Cr_2O_3. The general appearance of granulated furnace slag in section is shown in Figure 3 and Figure 4. The slag droplets as formed during granulation are brittle due to thermal shock, and on the outer surface there is often evidence of devitrification (with associated radial cracking) due to the depolymerising effect of water/steam granulation [9]. Certain of the large SCF slag granules sport a thin outer rim of slag spinel and magnetite – this is likely caused by oxidation of the slag surface during granulation. None of the surface effects extend more than a few micrometres into the slag granules, so they should not affect either the EPMA results or the bulk Mössbauer Spectroscopy results.

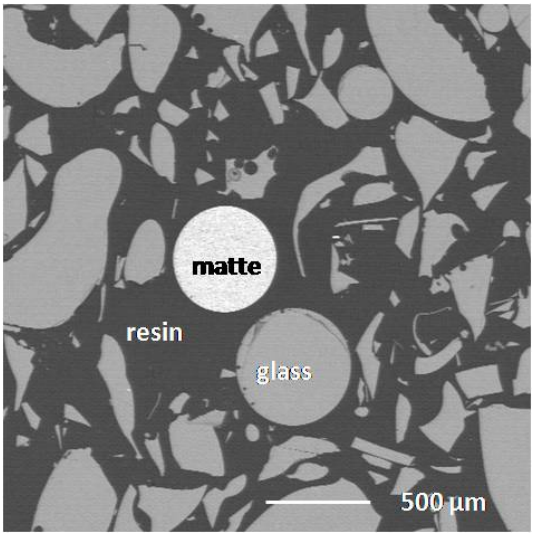

Figure 3. Backscattered electron (BSE) image showing granulated furnace slag in section. Most of the granules consist of silicate glass, but a sulphide matte granule has been entrained, possibly by tapping too close to the matte level. The black surrounding area is mounting resin.

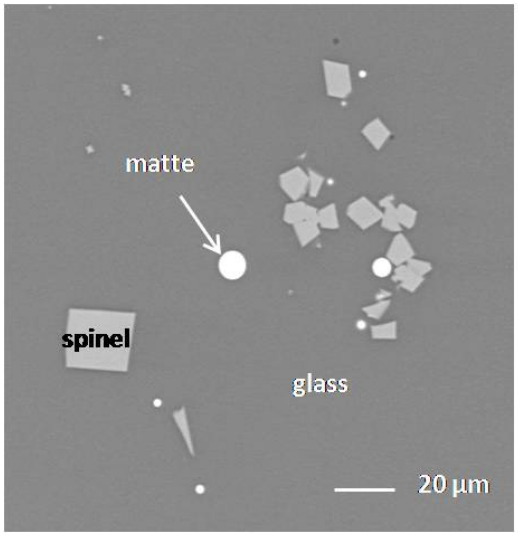

Figure 4. A higher magnification BSE image of a chromium-bearing furnace slag. Slag spinel crystals have formed and are associated with small entrained matte phases.

The compositions of the silicate glass in the primary furnace and SCF composites as determined by EPMA are shown in Table 3. SCF slag glass contains more iron and less magnesium than primary furnace slag. Note that the platinum-

group elements (PGEs) only occur in trace amounts in the silicate glass and these elements are therefore not detected by EPMA.

Table 3. Averaged results of EPMA of the silicate glass in mass %. Oxides are calculated by stoichiometry.

		Na_2O	MgO	Al_2O_3	SiO_2	CaO	TiO_2	Cr_2O_3	FeO	CoO	NiO	Cu_2O	S	Total
Primary	Average	0.460	22.32	5.90	51.95	4.00	0.260	1.84	12.79	0.019	0.083	0.078	0.176	100.12
Furnace	SD*	0.042	0.61	0.36	1.06	0.17	0.017	0.12	0.56	0.005	0.024	0.020	0.026	1.18
SCF	Average	0.287	7.74	3.26	38.53	1.45	0.136	1.17	46.41	0.175	0.244	0.345	0.369	100.18
	SD	0.020	0.32	0.21	0.94	0.11	0.010	0.31	0.84	0.040	0.116	0.084	0.071	0.67

*SD = standard deviation

Although the averaged glass analysis results shown in Table 3 are useful, more information can be obtained by producing scatter and contour plots showing the distribution of granule compositions; see Figure 5 and Figure 6. The data in these figures was obtained from individual EPMA of over 800 granules of primary furnace slag, and over 200 granules of SCF slag, with each analysis representing a moment of time inside the furnace or SCF. Figure 5 shows that the nickel oxide content of tapped slag silicate is far more tightly grouped in the primary furnace slag, whereas that of the SCF slag shows considerable variation over the month. This could be caused by variations in slag p_{O_2} and/or feed composition.

Figure 6 shows expanded contour plots of the primary and slag cleaning furnace slag. A number of interpretations can be made of plots such as this, provided that there has been no converter slag return to the furnaces, and that the slag tapping temperature has remained steady throughout the month. This plot suggests a slightly increased solubility of nickel in higher iron slags, and also shows a bimodal composition distribution. It has been established that this effect was caused by feed blending problems due to low stocks.

While these are not shown here, variation in slag basicity (calculated as $(MgO+CaO)/(Al_2O_3+SiO_2)$ for this operation), slag chromium solubility, and the relationship between base metal dissolution and slag sulphur content may also be inferred from scatter plots.

The large SCF slag granules selected for the equilibrium study were 1 to 2 mm in diameter. Some displayed (in addition to the surface features mentioned above) a degree of micro-crystallinity, so the electron beam was defocused to 5 µm during analysis. The results of EPMA and SEM-EDS analyses are shown in Tables 4 and 5.

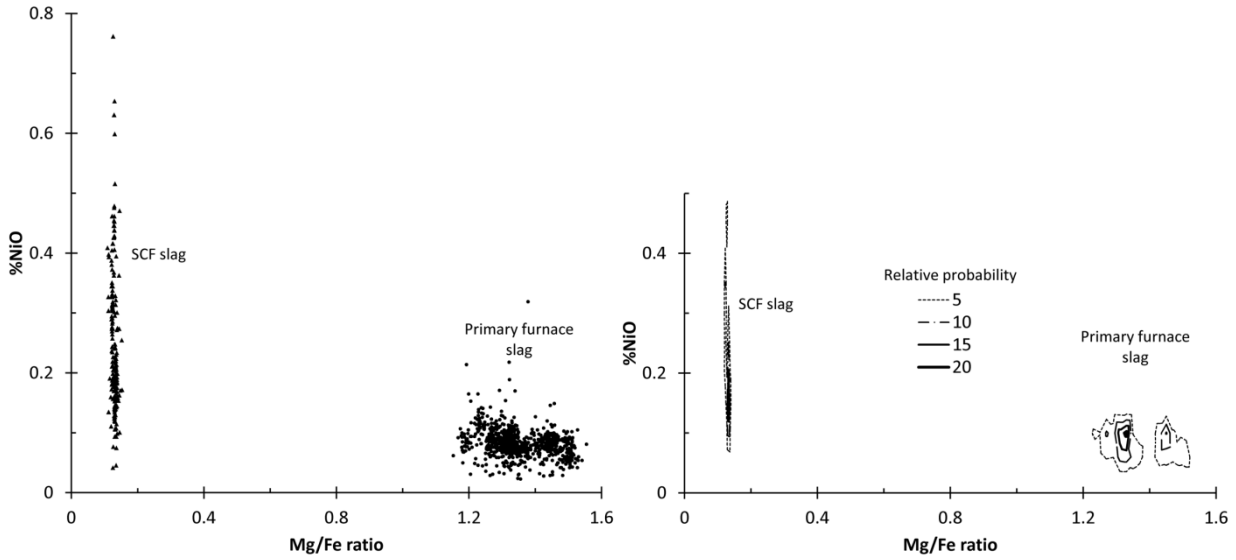

Figure 5. Scatter and contour plots showing the compositions of the primary furnace slag and SCF slag granules analysed by EPMA.

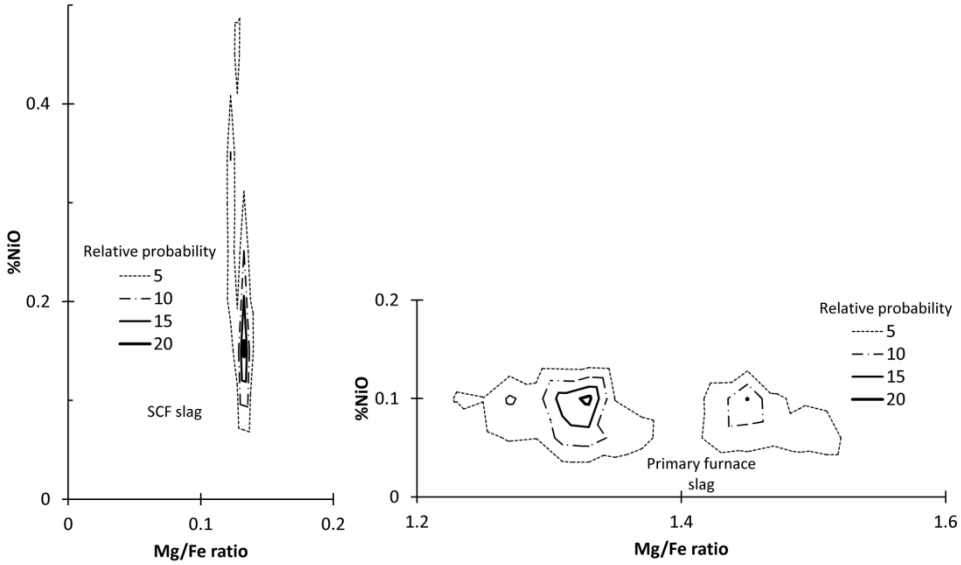

Figure 6. Enlarged contour plots showing the variation in composition of granules of slag cleaning furnace slag, and primary furnace slag.

Table 4. Averaged results of EPMA of ten large SCF slag granule silicate phases in mass %. Oxides are calculated by stoichiometry. Each average value was calculated from 10–15 point analyses; a grand average is also shown.

Granule	Na_2O	MgO	Al_2O_3	SiO_2	CaO	TiO_2	Cr_2O_3	FeO	CoO	NiO	Cu_2O	S	Total
1	0.309	7.60	3.62	39.69	1.71	0.131	0.473	46.50	0.211	0.226	0.275	0.686	101.12
2	0.289	7.55	3.24	38.97	1.45	0.130	0.714	47.21	0.246	0.359	0.391	0.581	100.84
3	0.290	7.06	3.23	38.18	1.44	0.130	0.942	48.50	0.247	0.324	0.353	0.578	100.98
4	0.280	8.09	3.16	40.07	1.44	0.136	1.672	45.38	0.139	0.173	0.311	0.576	101.15
5	0.267	7.95	3.16	40.48	1.47	0.132	1.186	45.67	0.136	0.132	0.257	0.590	101.17
6	0.308	7.68	3.52	38.71	1.66	0.137	0.846	46.43	0.217	0.330	0.325	0.664	100.53
7	0.306	7.29	3.41	38.49	1.48	0.135	0.801	47.66	0.167	0.166	0.308	0.594	100.51
8	0.285	7.45	3.32	39.51	1.61	0.127	0.375	48.00	0.218	0.148	0.246	0.645	100.64
9	0.315	6.99	3.83	40.08	1.97	0.138	0.602	45.56	0.174	0.129	0.228	0.788	100.47
10	0.323	7.65	3.57	38.98	1.70	0.135	0.448	46.71	0.203	0.165	0.263	0.681	100.49
Gr. ave.	0.297	7.53	3.40	39.22	1.59	0.133	0.806	46.76	0.196	0.215	0.296	0.638	100.79

Table 5. Averaged results of SEM-EDS area analysis of entrained matte phases in ten large SCF slag granules (mass % – results are normalized). Each average value was calculated from 10–50 analyses. A grand average is also displayed and compared to the composition of bulk matte, averaged over the month.

Granule	Fe	Co	Ni	Cu	S
1	13.3	1.3	48.3	14.5	22.5
2	12.8	1.3	45.3	17.3	23.4
3	15.5	1.4	44.5	16.8	21.9
4	27.0	1.6	36.8	12.5	22.0
5	23.8	1.5	34.9	16.9	22.9
6	13.5	1.3	44.5	17.1	23.6
7	16.2	1.5	41.6	19.0	21.6
8	14.9	1.6	45.4	15.4	22.7
9	18.2	1.6	42.9	15.2	22.2
10	16.1	1.6	45.8	14.0	22.5
Grand average	17.1	1.5	43.0	15.9	22.5
Tapped matte*	41.4	2.4	28.8	12.9	14.6

*From averaged chemistry results provided by the smelter.

The results of EPMA of the large granule silicate glass are in reasonable agreement with the SCF intragranular slag results shown in Table 3, with the possible exception of sulphur, which appears to be higher in the large granules. Since both sets of samples were measured using the same program and standards, this should not be an analytical artefact. Sulphur instability under the beam is known in sulphate samples, but this should not occur in silicates. Another possible explanation is that larger slag granules lose less sulphur to granulation water during quenching.

Examination of the results in Table 4 and Table 5 leads to the conclusion that the composition of the entrained matte phases is far more variable than that of the surrounding silicates (although, while the concentrations of the slag main components do not vary much, the concentrations of the base metal oxides do vary). Some implications of this are considered in the next section.

3.4 Modelling results

Comparison of base metal partition ratios with equilibrium

Previous work showed that the concentration of dissolved base metal oxides in the primary furnace slag approached equilibrium with the entrained matte droplets, taking the oxygen activity to be controlled by the buffer consisting of FeO in the slag and Fe in the matte droplets [5]. While the actual concentrations of dissolved cobalt oxide and nickel

oxide were close to this equilibrium, the copper oxide concentration was higher than expected, for the six-in-line primary smelting furnaces considered in that work. The work presented here tested whether similar relationships hold for the rather different conditions in a slag cleaning furnace.

Equilibrium predictions were on the basis of FactSage calculations of activities, activity coefficients and equilibrium constants. The activity of FeO in the slag and the activity coefficients of NiO, CoO and $CuO_{0.5}$ were calculated with the SlagA model of the FactSage FTOxid database. Activities of Fe, Cu, Ni and Co in the matte were calculated with the Matte model in the FactSage FTMisc database. All calculations were for 1450°C.

Although activities and activity coefficients in the slag were calculated separately for each slag composition, these values were very similar in all the slags, with the standard deviation less than 5% of the average value in all cases. In contrast, activities in the matte varied greatly. For example, the range of activity values of iron in the matte (solid reference state) was from 0.06 to 0.22, whereas the activity of FeO in the slag (solid reference) varied from 0.31 to 0.35. The large range of matte iron activity values significantly affects the predicted equilibrium partitioning of the base metals, which was calculated with the equilibria listed in Table 6.

Examples of activities and activity coefficients are given in Table 7. The "entrained matte" activities in Table 7 are for the "grand average" matte composition given in Table 5. Table 7 shows the much higher iron activity in the bulk (tapped) matte compared with the entrained matte. The significance of this is that, if base metal losses (as oxides) in the slag were governed by the composition of bulk matte, the high iron activity of the bulk matte would tend to give low nickel loss to the slag (as NiO; see reactions in Table 6). Predicted equilibrium dissolution of nickel, cobalt and copper oxides in the slag is given in Table 8. This demonstrates the expected effect, namely that equilibrium with the bulk matte would result in lower losses of base metals to the slag. In fact, nickel and cobalt in entrained matte appear to equilibrate with the nickel and cobalt oxide in the slag.

Table 6. Reaction equilibria considered when predicting dissolution of base metals. Reference states are pure solids, except for Cu (liquid reference state); T = 1450°C.

Reaction	Equilibrium constant
FeO + Co = Fe + CoO	0.059
FeO + Ni = Fe + NiO	0.011
$0.5FeO + Cu = 0.5Fe + CuO_{0.5}$	0.018

Table 7. Examples of activity and activity coefficients used in equilibrium calculations; T = 1450°C.

Activities in matte: (pure liquid reference state for Cu; pure solid for other metals)

	p_{S_2} (atm)	a_{Fe}	a_{Co}	a_{Ni}	a_{Cu}
Entrained matte	6×10^{-4}	0.11	0.013	0.29	0.16
Bulk matte	4×10^{-5}	0.51	0.029	0.26	0.28

Average activity coefficients and FeO activity in slag: (pure solid reference state for all oxides)

Species	CoO	NiO	$CuO_{0.5}$
$(\%MO_x)/a_{MOx}$	79	24	40

a_{FeO}=0.33

Table 8. Comparison of predicted equilibrium dissolution of base metals, for equilibration with entrained matte and bulk tapped matte; the actual base metal dissolution is close to that for equilibrium with entrained matte.

	%CoO	%NiO	$\%CuO_{0.5}$
Equilibrium with entrained matte	0.18	0.22	0.19
Equilibrium with bulk matte	0.09	0.04	0.16
Actual	0.20	0.22	0.30

While the values in Table 8 show the overall effects, analysis of slag and entrained matte in individual granules (as presented in Table 4 and Table 5) allow assessment of the extent to which local equilibrium is reached. To this end, Figure 7 compares predicted partition ratios with the measured values, for different granules. The partition ratios are (%M)/[%M], where (%M) is the mass percentage of element M in the slag, and [%M] its mass percentage in the matte. The observed cobalt partition ratio can be seen to be close to the predicted value (for equilibrium between entrained matte and bulk slag), and to vary with iron activity as expected. (Changes in iron activity change the predicted cobalt partition *via* the reaction given in Table 6.) For nickel, the values agree on average, but with significant scatter. This difference in the variability of nickel and cobalt partition ratios (relative to predictions) may simply result from their relative concentrations in the matte: nickel is the main constituent of the entrained matte, so variations in its concentration affect the activity of iron; in contrast, cobalt is a minor constituent of the entrained matte. (Higher nickel contents in the matte imply lower matte iron contents, and hence higher nickel partition ratios, based on the FeO-Ni reaction in Table 6.) Partitioning of copper to the slag is consistently greater than equilibrium predictions, in line with previous work [5]; it is not clear whether this deviation is a mechanistic effect, or simply reflects the inherent uncertainty of the solution models.

These results show local equilibration of base metals in entrained matte with the bulk slag, in the slag cleaning furnace (as was also previously found for the primary smelting furnace). In addition, variations in partitioning of base metals in the slag (probably reflecting changes in furnace conditions over time) do correlate with variations in entrained matte composition.

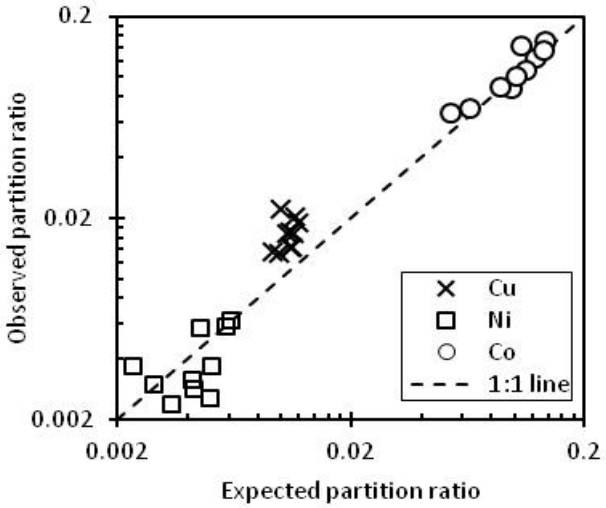

Figure 7. Comparison of observed and predicted partition ratios of copper, nickel and cobalt between matte and slag, based on equilibrium between matte droplets and slag.

Partial reaction between concentrate, converter slag and carbon

The calculations show equilibration between dissolved nickel oxide and cobalt oxide in the slag cleaning furnace (SCF) slag and the entrained matte droplets, assuming the oxygen activity to be controlled by the $(FeO)_{slag}/[Fe]_{entrained\ matte}$ buffer. The resulting high nickel content of the entrained matte droplets (Table 5) negatively affects nickel recovery, because a significant proportion of the nickel loss in the SCF slag appears to be in the form of matte droplets: Table 2 shows the total nickel content of the SCF slag to be 0.34%, whereas microprobe analysis of the slag indicates a dissolved nickel content of 0.17% (Table 4); hence approximately half of the nickel loss to the slag is as entrained matte droplets. The fundamental question is what determines the composition of the entrained matte droplets. The entrained matte is very different in composition from the bulk (tapped) matte (Table 5), especially in sulphur content (22.5% in entrained matte, 14.6% in bulk matte), and Ni/Fe mass ratio (2.5 in entrained matte, 0.7 in bulk matte).

The high nickel content and relatively high sulphur are consistent with the entrained matte having formed by resulphidation reactions such as

$$(FeS)_{matte} + (NiO)_{slag} = (NiS)_{matte} + (FeO)_{slag}.$$

Equilibrium of this reaction lies well to the right (K = 20 at 1450°C, for pure liquid reference state for all species). Reaction of the concentrate (source of FeS) with the converter slag (containing NiO) would hence tend to give a high Ni/Fe ratio in the matte reaction product. Addition of carbon would cause reduction of iron oxide to metallic iron, hence giving a lower Ni/Fe ratio (and a lower sulphur content) in the matte.

To test whether these predictions agree quantitatively with the observed compositions, equilibrium compositions were calculated using FactSage (for a temperature of 1450°C), considering as possible phases the FToxid-SLAGA model for the slag, FTmisc-MATT for liquid matte, FTmisc-BCCS and FTmisc-FCCS for solid alloy phases (which may form if the sulphur content of the product is too low), and gaseous species (mainly CO, CO_2 and SO_2). Compositions considered in the calculations are listed in Table 1. Pure carbon was considered as reductant. In the operation considered here, the mass ratio of concentrate to converter slag is approximately 0.47, and of carbon to converter slag approximately 0.019-0.023.

Some results are shown in Figure 8. Figure 8 a) demonstrates that both concentrate additions (contributing to resulphidation) and carbon additions (contributing to more reducing conditions) promote nickel recovery. The actual SCF feed ratios (concentrate/[converter slag] = 0.47 and C/[converter slag] = 0.019-0.023) are approximated by the intersection of the vertical dot-dash line and the curves for C/[converter slag] = 1.9% in Figure 8; the equilibrium nickel recovery should be greater than 95%. As noted earlier, the actual nickel recovery is approximately 85%, which is less than the equilibrium recovery because of departure from overall equilibrium in the furnace, and because of physical entrainment of high-nickel matte droplets.

In Figure 8 c), the actual sulphur content of the bulk matte (horizontal broken line labelled "Bulk matte") can be seen to agree approximately with the equilibrium prediction (intersection of vertical dot-dash line, and curve for C/[converter slag] = 1.9%). However, this agreement is really based on the overall mass balance (the sulphur content of the bulk matte largely depends on dilution of the sulphur in the matte by iron produced by carbon additions); the actual nickel content of the bulk matte is much lower than the equilibrium prediction (Figure 8 b).

Figure 8 b) and c) give some indication of how the composition of the entrained matte droplets can arise: the entrained matte may form by reaction to equilibrium between the converter slag, carbon and concentrate, but in ratios different from the overall feed ratios. Figure 8 b) and c) indicate that the high Ni/Fe ratio and high sulphur content of the entrained matte correspond to equilibration for a concentrate/[converter slag] ratio of approximately 0.8 (approximately twice the actual feed ratio), and a carbon/[converter slag] ratio of approximately 1.5 (somewhat lower than the actual ratio). This might reflect inadequate mixing of the feed materials in the slag cleaning furnace; one possible mechanism behind non-equilibration is discussed in the next section.

As a separate point, the onset of alloy formation was predicted as part of the equilibrium calculations. Formation of solid alloy (at low sulphur levels) would be undesirable, since the alloy would tend to sink to the bottom of the furnace, trapping valuable metals. The lowest concentrate/[converter slag] ratio along each of the curves in Figure 8 indicates the onset of alloy formation. As expected, higher carbon/[converter slag] ratios (producing more metal) require larger concentrate additions to avoid alloy formation; Figure 8 c) shows that alloy formation is avoided if the sulphur content of the matte is higher than approximately 11.5% (at 1450°C); the actual bulk matte sulphur content (14.6%) is safely above this.

Possible reaction mechanism

Eksteen [10] recently suggested that the diameter of matte droplets, draining from unmelted concentrate oxides into slag, may be several millimetres; such large diameters follow from droplet size correlations for liquid draining from a packed bed [11]. Large-diameter matte droplets would drain rapidly through the slag, and hence would be unlikely to equilibrate during settling. In contrast, the much smaller entrained matte droplets settle slowly, allowing the observed equilibration. Added reductant floats on the slag, and likely reacts to completion. The simplest reaction scheme which includes all these elements is illustrated in Figure 9: the majority of the sulphides in the concentrate drain to the bulk matte; a small fraction of the sulphides form small (entrained) droplets which equilibrate with the slag which forms by reaction between the reductant and the converter slag. Reaction between the reductant and slag forms an alloy product which settles to form part of the bulk matte. (This is undoubtedly an over-simplified view of the reactions in the furnace, but serves as a base case.) The compositions resulting from this reaction scheme were evaluated with the FactSage databases as mentioned, using the ChemSheet spreadsheet add-in [12]. The results of the calculation are approximate, because the models for the solid and liquid alloy phases are not optimised over the range of compositions expected to form. For feed ratios of 477 kg concentrate and 23 kg carbon per ton converter slag, assuming 90% of the concentrate sulphides to drain directly to the bulk matte, the resulting bulk matte composition is found to be 41% Fe; 31%

Ni; 14% S; 12% Cu; 2% Co, close to the actual bulk matte (Table 5); the (oxidic) base metal content of the bulk slag is also close to that observed, with Fe^{3+}/Fe_{tot} = 0.04 (similar to the measured value of 0.06). While the composition of entrained matte (resulting from equilibration of 10% of the sulphides from the concentrate with the slag) had a Ni/Fe ratio of the right order (2.2, compared with the actual value of 2.5), the calculated sulphur content of the entrained matte was too low (12% compared with the actual 22.5%).

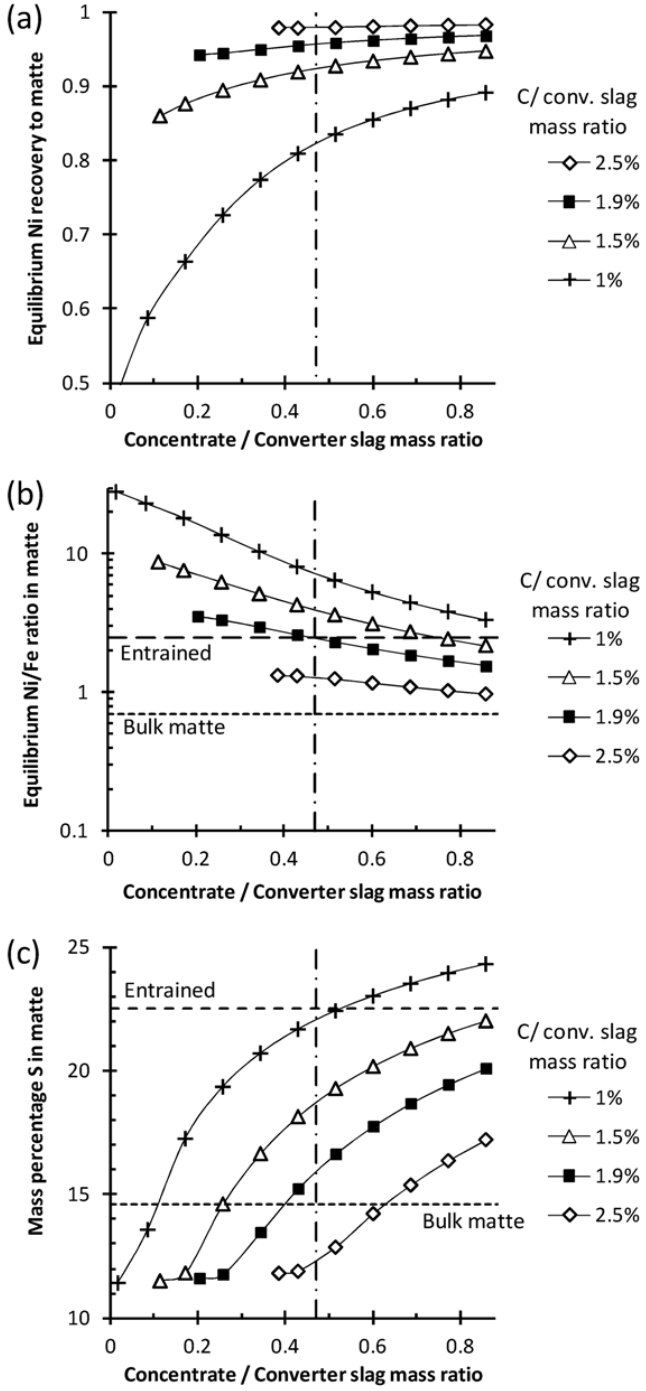

Figure 8. Predicted equilibrium compositions, for reaction of converter slag, concentrate (compositions as in Table 1) and carbon, in various ratios, at 1450°C. Solid metallic alloy forms at concentrate ratios less than the point at which each curve terminates.

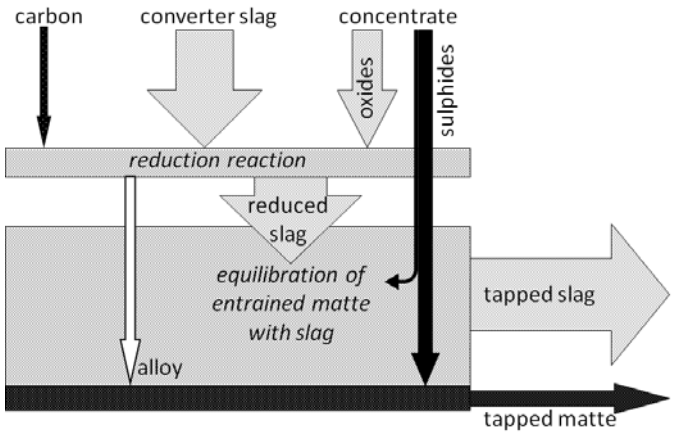

Figure 9. Possible reaction mechanisms in the slag cleaning furnace.

If the reaction scheme of Figure 9 did hold, this would have important implications for control of metal recovery in the slag cleaning furnace, as also indicated by the calculated mass balance for this reaction scheme (Figure 10). According to this, most of the nickel, copper and cobalt in the bulk matte are recovered by reduction from the converter slag, whereas all of the sulphur and most of the iron are from the added concentrate. Approximately half the added carbon serves to reduce Fe^{3+} to Fe^{2+}, and hence a small increase in the carbon input should result in a substantial increase in base metal recovery.

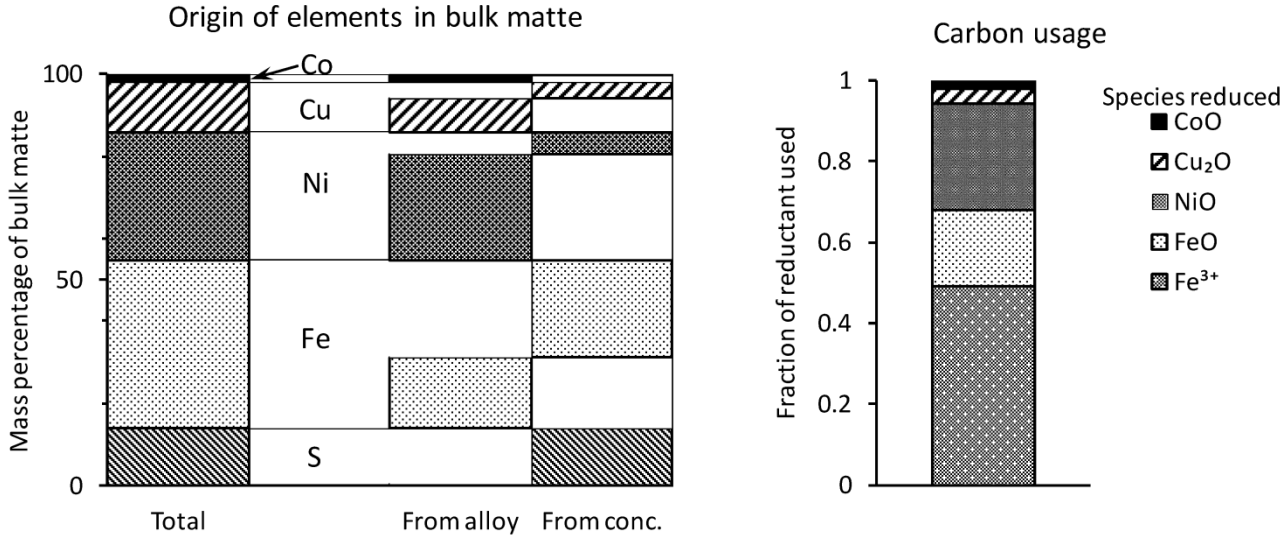

Figure 10. Calculated mass balance for reaction scheme of Figure 9, showing the origin of elements in the bulk matte (left), and carbon-consuming reactions (right).

4. Conclusions

The study shows that techniques such as bulk sample chemistry, electron beam microanalysis and Mössbauer Spectroscopy may all be combined successfully to characterize granulated platinum slags and modelled to provide

information about conditions inside the furnace. As in the primary smelting (six-in-line) furnace, base metal oxides in the SCF slag equilibrate with the entrained matte droplets. Significant variations in the base metal content of individual slag granules correlate with variations in the composition of entrained matte in those droplets. This suggests that local slag-matte equilibrium is with entrained matte. However, overall metal partitioning between slag and matte is far out of equilibrium with the bulk (tapped) matte. These compositions may arise from a reaction scheme involving rapid settling of most of the concentrate sulphides to the bulk matte.

Acknowledgements

The authors would like to thank Platinum for permission to publish this work, and all the staff at Platinum Head Office and Smelters, and at Research, who have assisted with this project, especially Rodney Hundermark (Platinum). The assistance of Christian Reinke, of the University of Johannesburg, is also gratefully acknowledged.

References

[1] J. Nell. Melting of platinum group metal concentrates in South Africa. *J. S. African Inst. Mining and Metall.*, 2004, 104(8), p423-428.

[2] L.A. Cramer. The extractive metallurgy of South Africa's platinum ores. *J.O.M.*, 2001, 53(10), p14-18.

[3] M. Jacobs. Process description and abbreviated history of Anglo Platinum's Waterval Smelter. In R.T. Jones (ed.), *Southern African Pyrometallurgy 2006*, Southern African Institute of Mining and Metallurgy, Johannesburg, South Africa, p17-28.

[4] R.J. Hundermark, S.B. Mncwango, L.P.vS. de Villiers, L.R. Nelson. The smelting operations of Anglo American's platinum business: An update. In R.T. Jones and P. den Hoed (eds), *Southern African Pyrometallurgy 2011*, Southern African Institute of Mining and Metallurgy, Johannesburg, South Africa, p295-307.

[5] L. Andrews and P.C. Pistorius. Nickel, copper and cobalt distribution and equilibria in Anglo Platinum furnace slags. *Mineral Processing and Extractive Metall. C*, 2010, 119(2), p52-59.

[6] L. Andrews, P.C. Pistorius and F.B. Waanders. Electron beam and Mossbauer techniques combined to optimise base metal partitioning in the furnace. *Microchim. Acta*, 2008,161, p445-450.

[7] L. Andrews. Microprobe characterisation of slag: Boosting compositional data. *Proc. Microscopy Soc. S. Africa*, 2011, 41, p82.

[8] C.W. Bale, P. Chartrand, S.A. Degterov, G. Eriksson, K. Hack, R.B. Mahfoud, J. Melançon, A.D. Pelton and S. Petersen. FactSage thermochemical software and databases. *Calphad*, 2002, 26, p189-228.

[9] E.T. Turkdogan, Reaction of gases and vapours with polymeric melts. In *Physicochemical properties of molten slags and glasses.* The Metals Society, London, 1983, p201.

[10] J.J. Eksteen. A mechanistic model to predict matte temperatures during the smelting of UG2-rich blends of platinum group metal concentrates. *Minerals Engineering*, 2011, 24, p676-687.

[11] A.F. Seibert and J.R. Fair. Hydrodynamics and mass transfer in spray and packed liquid–liquid extraction columns. *Industrial and Engineering Chemistry Research*, 1988, 27, p470–481.

[12] P. Koukkari, K. Penttilä, K. Hack and S. Petersen. ChemSheet – an efficient worksheet tool for thermodynamic process simulation. *Microstructures, mechanical properties and processes – computer simulation and modelling*. Proceedings of the 6th European Conference on Advanced Materials and Processes, 1999, p323-330.